9. PARTICIPATION IN THE FUSION TECHNOLOGY PROGRAMME

Carlos Varandas and J.Carvalho Soares (Heads), R.C. Pereira, N. Cruz, C. Correia, M.F. Silva, E. Alves, M.R. Silva, A. Melo, L. Alves, A. Paul

9.1. INTRODUCTION

The Portuguese participation in the Fusion Technology Programme included in 2000 the following projects:

- Fusion materials characterization and surface ion beam modifications
- Beryllium pebble bed electrical resistivity in the presence of ionising radiation
- SiC SiC ceramic composites
- Qualification of high performance steels
- Monitoring system for a laser-in-vessel viewing system

carried out in the frame of Underlying Technology (the first project) and Technology Tasks (the last four projects), by "Instituto Tecnológico e Nuclear" (ITN) (the first four projects) and "Centro de Fusão Nuclear" (the last project).

9.2. FUSION MATERIALS CHARACTERIZATION AND SURFACE ION BEAM MODIFICATIONS

Some ITN facilities (a research fission reactor, a VanderGraff accelarator and an ion beam probe) have been used to test materials for fusion applications.

9.3. BERYLLIUM PEBBLE BED ELECTRICAL RESISTIVITY IN THE PRESENCE OF IONISING RADIATION (Task TW0-T431/01)

9.3.1. Main activities

The main activities made in 2000 were:

- Design and construction of the experimental set-up for electrical resistivity measurements
- Investigation of the electrical properties of a Be pebble bed
- Study of the neutron activation of a single Be pebble
- Beginning of the elaboration of the final report.

9.3.2. Main results

The electrical properties of a Be Pebble Bed have been investigated. It was observed that the oxide scale present on the beryllium pebble surfaces, and the limited contact between the pebbles due to the bed porosity led to a resistivity which is about two orders of magnitude higher than that of steel. However the performed measurements were done in air. It is now expected that the beryllium shall be accommodated in a typical purge gas environment, using He + 0.1 % H as foreseen in the blanket design, which could have an impact on the oxygen distribution on the surface. From experiments with electrical insulators in helium environment, it is known that He atoms can be ionised by radiation, and thereby influence the electrical properties of the system. It will be checked whether similar phenomena have to be faced in a beryllium pebble bed.

The Be pebbles that are going to be used are from a different manufacturer than the ones previously used. These new Be pebbles were produced by NGK company (Japan). Spherical beryllium pebbles with 1mm diameter constitute the whole lot and they present a better degree both in size uniformity and surface irregularities. Nevertheless, the impurity contents and distribution as well as the surface oxidized layer should be evaluated. For that, ion beam analysis techniques are going to be used. A first study was done using the nuclear microprobe, which allowed us to investigate in detail the surface avoiding the influence of the curvature of the pebbles on the analysis. A 1.5 μm – 3 μm H^+ beam was used to scan the pebbles surface and the backscattered particles and X-rays were collected with a surface barrier and Si(Li) detectors, respectively. The typical results are shown in the figures below. The elemental maps reveal the homogeneity of the Be and some inclusions of Ca due to some surface contamination (Fig. 9.1). The main impurities in the pebbles were detected by the PIXE technique were Ti, V, Cr, Mn, Fe, Ni and Cu (Fig. 9.2a). We notice also the presence of U with concentrations below 14 μg/g. This result led us to start a new study of a large ensemble of pebbles in order to get a reliable value for the concentration of this element in the pebbles. The detailed study of the oxide scale in the pebbles, determined from the RBS spectrum is under evaluation (Fig. 9.2b).

Neutron activation analysis of a single Be pebble was used to confirm the presence of uranium in the pebbles and allowed to detect also the presence of gold in trace amounts (Fig. 9.3).

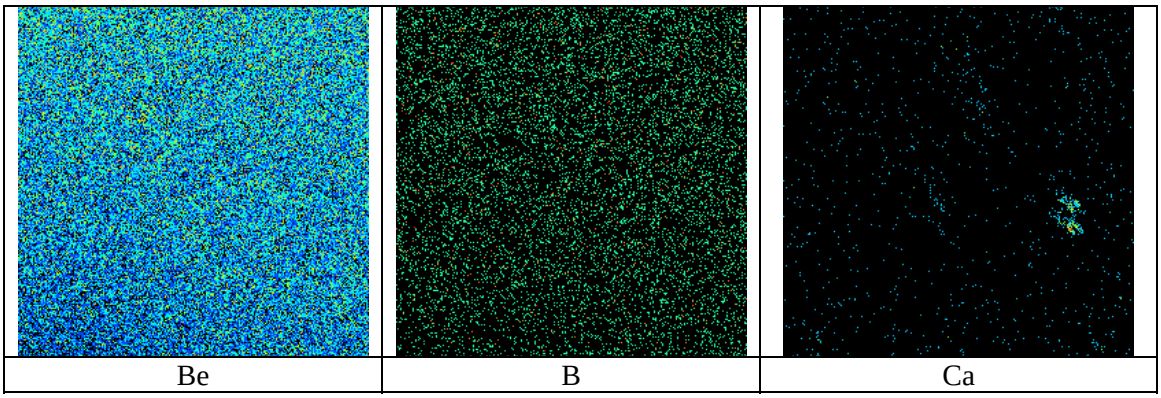

Fig. 9.1 – PIXE and RBS elemental maps obtained from a 500 μm^2 proton beam scan on the Be pebbles

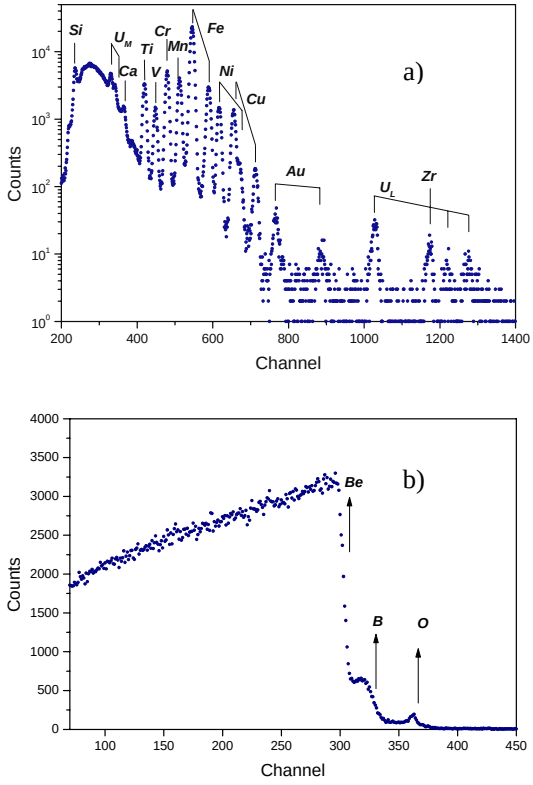

Fig. 9.2 – PIXE and RBS spectra of a Be NGK pebble

The experimental set-up for electrical resistivity measurements was designed and final construction and assembly is being carried out. In this new set-up a constant current of 250 mA will be applied and the voltage drop along the Be pebble bed measured for different loads. The same set-up will be used to apply a fix load into the pebble bed and fill with the gas mixture (He + 0.1 % H). It was supposed that the measurements could also be carried out during neutron irradiation which can be compromised due to the presence of U in the Be pebbles.

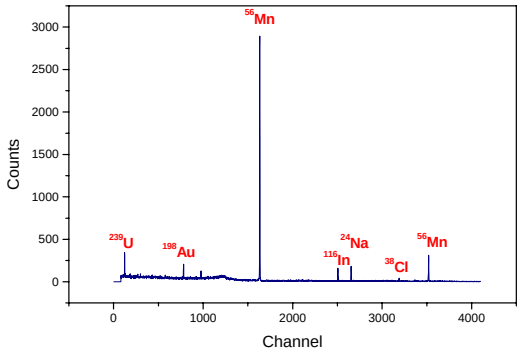

Fig. 9.3 – Neutron activation analysis spectra of a single NGK Be pebble

9.4. SiC SiC CERAMIC COMPOSITES (TW0-TTMA-001)

9.4.1. Main activities

The following main activities have been carried out:

- Investigation of the chemical behaviour of 3D SiC/SiC composites (produced by CERASEP) when exposed to Li_4SiO_4 or Li_2TiO_2 during 216 and 1000 hours at 800 ^oC. These studies have been based on simultaneous PIXE and RBS spectra collected using proton micro-beams (≅ 3 μm spatial resolution) with energies of 1.7 MeV, 1.75 MeV and 2.0 MeV.
- Analysis with ion micro-beam techniques of ceramic breeders that were in contact with the SiC composites.

9.4.2. Main Results

The chemical behaviour of 3D SiC/SiC_f composites (produced by CERASEP) when exposed to Li_4SiO_4 or Li_2TiO_3 during 216h and 1000h at 800ºC was further investigated. It was previously reported a surface oxidation in all the studied composites as well as a Li diffusion and a strong C depletion in

the front layer. In this work, simultaneous PIXE and RBS spectra were collected using proton micro-beams (~3 µm spatial resolution) with energies of 1.7 MeV, 1.75 MeV and 2.0 MeV. This will not only give information on different depths of analysis but also enhance the surface carbon RBS signal through the carbon resonance at 1.75 MeV.

Fig. 9.4 shows the obtained Si and Ti X-ray maps for the sample exposed during 1000h to Li_2TiO_3, as well as the elemental maps for Si and Fe of the virgin sample, obtained at 1.75 MeV. Also presented in the same figure are the RBS spectra obtained from the marked points in the scan map at the proton energies used. The elemental maps of Si present some surface topography information and by comparison with the virgin sample is immediate to observe the induced surface alterations. The Fe contamination of the virgin samples is again revealed, while some particular features of Ti rich clusters are also observed. The RBS spectra obtained show the huge influence of getting information on the C content by working above or bellow the resonant energy. The two point spectra obtained also show very different chemical behaviour where the zone with intense Si is also the zone with intense C endeavouring a C-Si bounding that was not observed in previous XPS experiments.

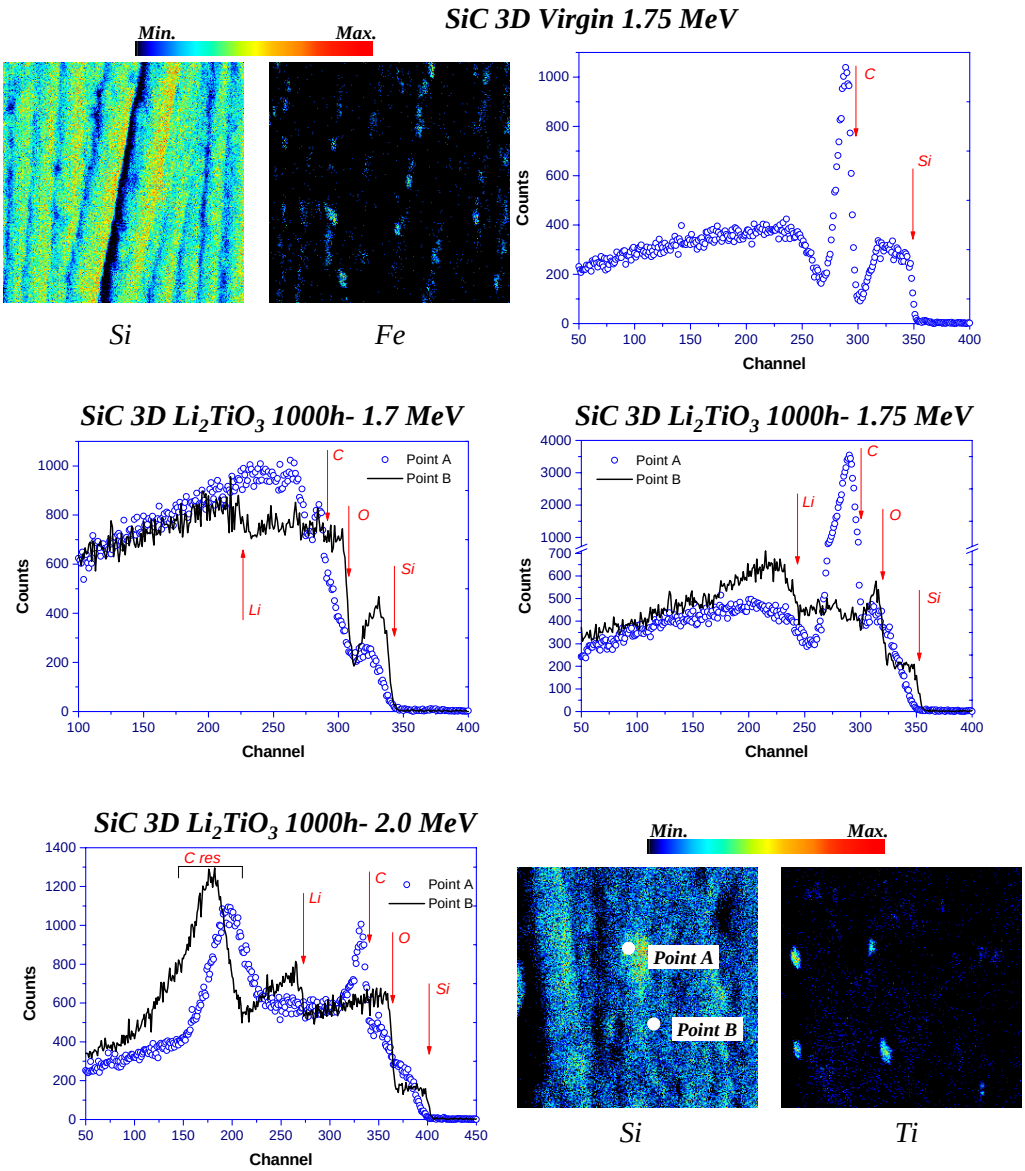

Fig. 9.4 - 500µm² scan elemental maps of Si and Fe for the SiC virgin sample and of Si and Ti for the SiC sample exposed during 1000h to Li_2TiO_3. Virgin sample shows the original Fe impurities and the exposed samples the formation of Ti precipitates. Also shown are a RBS sum spectrum obtained from the virgin sample at a proton energy of 1.75 MeV, and the RBS spectra from point A and B (at 1.7 MeV, 1.75 MeV and 2.0 MeV proton beam energy) of the sample exposed to Li_2TiO_3.

The results obtained from the RBS spectra of the analysed points (having chosen regions with intense Si and others with lower Si content) can be summarised as follows:

a) Sample exposed to Li_4SiO_4 for 216h: strong depletion of C in the first 5µm accompanied by Li and O diffusion up to 10µm;
b) Sample exposed to Li_4SiO_4 for 1000h: Li and O diffusion increase up to 30 µm and strong depletion of C is observed in the first 15 µm; although point to point analysis present small differences in the extent and strength of the induced chemical reactions, no distinct chemical behaviour could be observed;
c) Sample exposed to Li_2TiO_3 for 216h: both analysed points lead to alterations in the first 2-2.5µm and the depletion of C is so important that in the affected layer C could only be detected for energies above the resonant value (1.75 MeV);
d) Sample exposed to Li_2TiO_3 for 1000h: the two points chosen for analysis revealed very distinct behaviour – point B has long range surface alteration (25 µm) with diffusion of Li and O; C not detected in the first 8µm, strongly depleted in the following 9µm and increased concentration in the last 7µm; point A presents oxidation of only the first 1.5µm accompanied by a very pronounced increase of C (roughly, a factor of 10 relative to Si abundance) and small diffusion of Li and O in the rest of the material.

The very strong increase of C in point A of this last sample and the observation of the RBS spectra taken at 1.75 MeV proton energy endeavours the possibility of generating direct carbon RBS maps. Those maps are presented in Fig. 9.5 for the samples exposed to Li_2TiO_3. Also shown in Fig. 9.5 are the RBS spectra obtained in the masks 1, 2, 3 and 4. The RBS spectra of those masks confirm that the diffusion of Li and O is reduced in the zones with high amounts of C endeavouring the possibility of some kind of surface treatment for chemical passivation.

As new 3D SiC/SiC_f composites will be available, studies will be carried out to check for impurity content and surface distribution. Chemical stability to new breeding materials in fusion relevant conditions will also be performed.

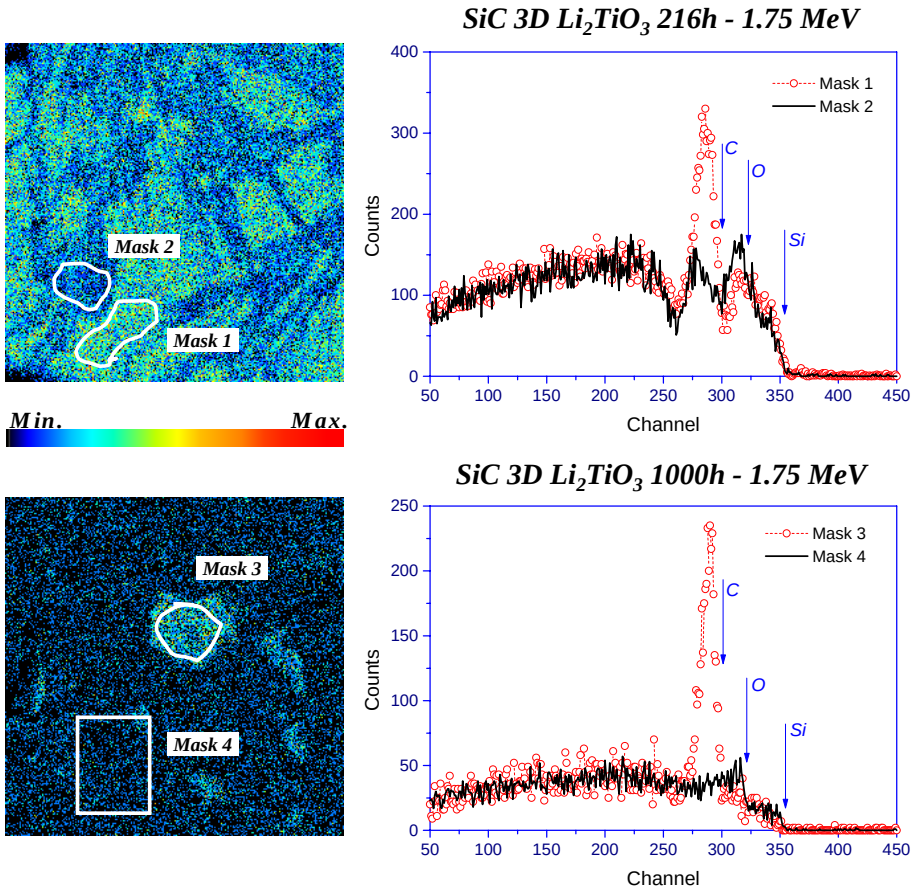

Fig. 9.5 - 500 µm2 scan elemental maps of C obtained from the samples exposed to Li_2TiO_3 as well as the RBS spectra obtained in each of the referenced masks.

The ceramic breeders that were in contact with the SiC composites (Li_4SiO_4 and Li_2TiO_3 pebbles) in the conditions referred in the previous section were also analysed by ion micro-beam techniques. The virgin material is white coloured whereas in each of the exposed lots, dark and white pebbles could be observed.

As can be seen in Fig. 9.6a, C is present in the Li_4SiO_4 pebbles surface even for the virgin sample and they do not show any reaction with C from the SiC material. The presence of C in the front layer of the material is enhanced by the analysis with protons at the C resonance energy of 1.75MeV as can be observed in Fig. 9.6b. Fig 9.6a also shows the formation of a thin Si surface layer with ~100 nm thickness. The material is not homogeneous as different pebbles present large differences in the Si.

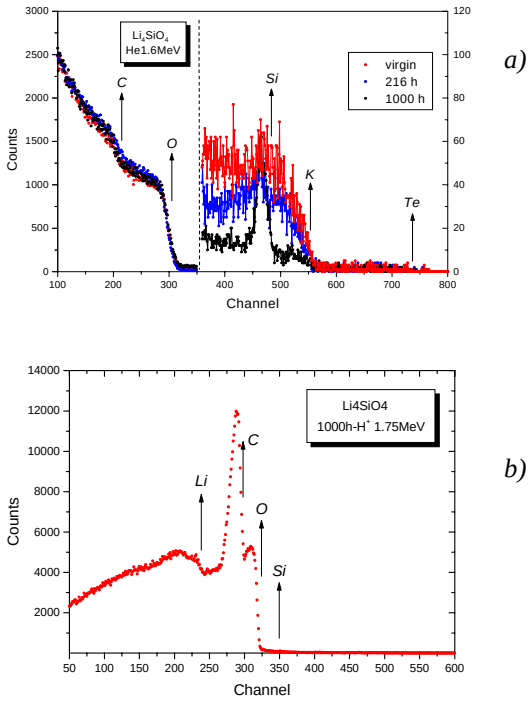

Fig. 9.6 – µRBS of Li_4SiO_4 ceramic pebbles: a) virgin and exposed samples analysis with 1.6 MeV He^+ beam show the formation of a Si surface layer; b) RBS C signal is enhanced through the use of a proton beam of 1.75 MeV.

The Li_2TiO_3 ceramic pebbles do not show any significant change in composition from the virgin and the annealed samples (Fig. 9.7a). Only at the proton resonant energy a small amount of C can be found in the surface layer (Fig. 9.7b) that, nevertheless, can be responsible for the observed colour transition from white to brown in the virgin and annealed samples.

The chemical behaviour and compatibility with structural material in fusion relevant condition will be further investigated.

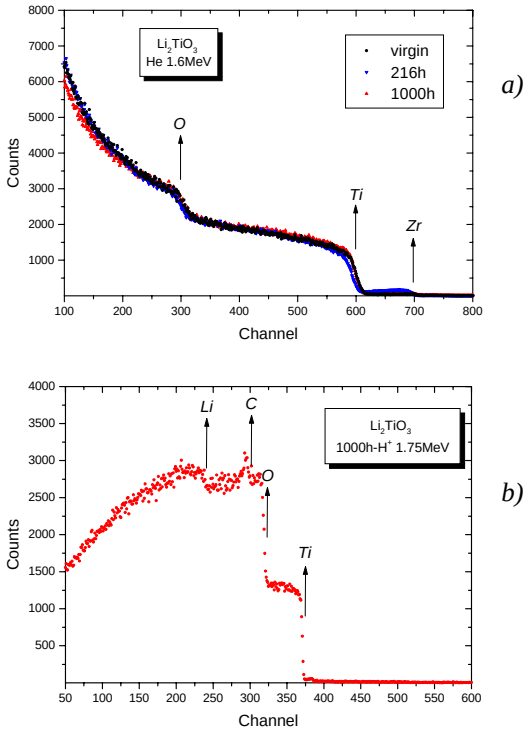

Fig. 9.7 - µRBS of Li_2TiO_3 ceramic pebbles: a) virgin and exposed samples analysis with 1.6 MeV He^+ beam; b) RBS spectra obtained with a proton beam of 1.75 MeV for the sample exposed during 1000h.

9.5. QUALIFICATION OF HIGH PERFORMANCE STEELS (TW0-TTMS-006)

9.5.1. Introduction

The following main activities have been performed:

- Fabrication of several experimental alloys in vacuum/gas induction furnace in 100 gr ingots alloy compositions have been made starting from the F-82H composition. Variations in the composition of the other elements will be pursued in order to increase the high temperature resistance.
- Fabrication of U-doped standards, starting from the F-82H alloy doped with low U levels.

9.5.2. Main results

The work undertaken has been centred in the fabrication of low activated ferritic martensitic alloys and U-doped standards.

Several experimental alloys were fabricated in vacuum/gas induction furnace in 100g ingots. Alloy compositions are made starting from the F-82H composition, which will be used as reference. Variations in the composition of other elements will be pursued in order to increase the high temperature resistance. Ranges for the alloy elements are: Cr 7.7-13 wt%, Si 0.03-0.8 wt%, N 0.008-0.02 wt%, W 0.8-2 wt%, Ta 0.02-0.1 wt%, V 0.15-0.4 wt%, Ti

0.001-0.1 wt%. C will be kept constant at 0.09 wt%. Those alloys are actually being characterised in the as-cast condition.

U-doped standards are fabricated in the same way as the experimental alloys. F-82H alloy has been doped with low U levels (μg/g). Initially metallic U was directly added to the rest of the elements to be melted but U segregation to the slag prevented its incorporation into the alloy. In order to increase the solubility of U in the ferritic-martensitic alloy, some Sn was added. The obtained results show an increase in the U content of the alloy. Actually the U levels obtained, as determined using PIXE, are 56 μg/g using metallic U, with an efficiency of 0.005 ($U_{measured}$/ $U_{expected}$) and 47 μg/g when Sn was added with an efficiency five times higher than the previous.

During the next six-month period, the experimental alloys will be characterised in the as-cast and in the normalised and tempered conditions using a variety of techniques (such as optical and electron mettalography, XRD, thermogravimetry) in order to investigate which of the compositions is more adequate for fabrication in larger heats (600 g ingots).

Taking into account the increase of the U solubility in F-82H alloy, U-doped standards will be made starting from U inter-metallic. U_6Mn and U_3Si are good candidates because both Si and Mn are present in the composition of the alloy and small additions will not affect the final structure. Characterization of the inter-metallics and alloys will be also performed.

9.6. MONITORING SYSTEMS FOR LASER IN-VESSEL VIEWING SYSTEMS (Tasks D325 (R27) and TV-018-2)

9.6.1. Introduction

This project, carried out in collaboration with ENEA-Frascati, aims the development of monitoring systems for the laser in-vessel viewing systems of JET and ITER-FEAT.

9.6.2. Main activities

The following main activities were carried out in 2000:

- Design of the new system and development of the new software for the JET tool.
- Installation of this system at ENEA Frascati.
- Design of the architecture of the monitoring system for the ITER-FEAT tool and definition of the technical characteristics of the VME modules for control and data acquisition.
- Beginning of the design of these VME modules
- Beginning of the call for tender for the VME system for the ITER-FEAT tool.

9.6.3. Monitoring system for the ITER-FEAT tool

The control and data acquisition system for the ITER-FEAT in-vessel vision system (Figure 9.8) is an improvement of a similar system that has been developed for the JET laser in-vessel viewing system.

The main upgrades and new features are: (i) the MC68060 microprocessor was changed to a PowerPC604R based CPU in order to guarantee the sustained data transfer rates to the network of 2Mbyte/s for 100 kHz pixel clock; (ii) the OS9 operating system was substituted by LynxOS, to face the network performance and real time demands; (iii) the three modules used in the previous system were reduced to two, leading to a more reliable system and reducing the assembling and testing time; (iv) programmable motor speed depending on angular position of the prism in order to increase the accuracy in the zone of interest and to minimise the overall acquisition time; and (v) amplitude and phase analog information from the radar electronic unit in order to have redundant information.

The IVVS control and data acquisition system is composed by a supervisory workstation connected by a 100 Mbit/s Ethernet channel to a 12-slot backplane (P1, P2) VME crate, housing a PowerPC604R based CPU, with 64 MB RAM, 9 GB hard disk and running LynxOS, as well as two on-site developed modules:

- The intelligent control and data acquisition (CADA) module, dedicated to control the laser operation for the in-vessel scanning and to acquire and store the in-vessel image;
- The intelligent monitoring module, dedicated to monitor external variables and to signal predefined error situations.

Fig. 9.9 depicts a block diagram of the VME system. LynxOS is an UNIX compatible, POSIX-compliant, operating system, used in time critical applications where predictable real-time response is necessary.

For CADAS three levels of software were developed:

- A lower level software that runs in the two on-site developed modules hosted by the 32 bit, 50 MHz floating-point, TMS320C31 Digital Signal Processor (DSP);

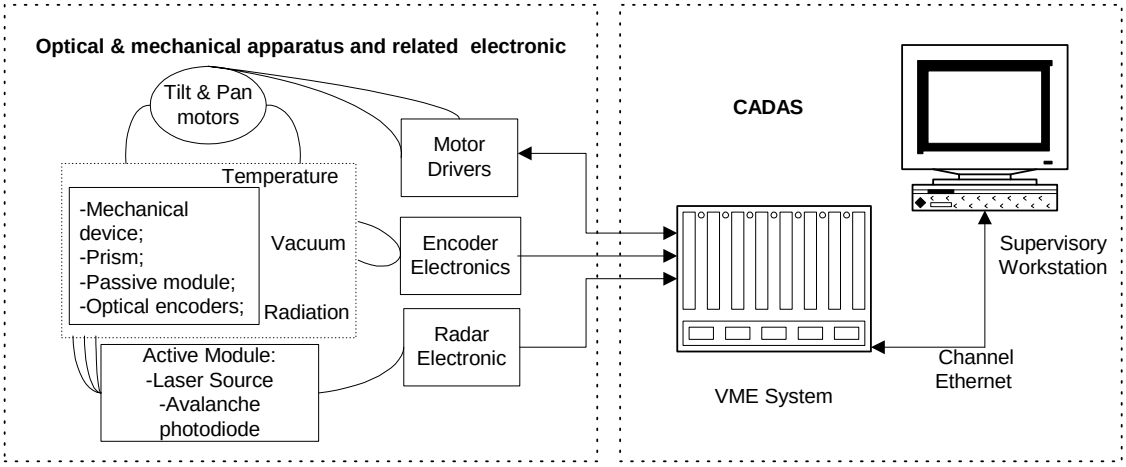

Fig. 9.8 – Block diagram of the in-vessel viewing system

- A middle level software (TCP/IP Server Application) that runs in a PowerPC board, hosted by a PPC 400 MHz microprocessor running the LynxOS operating system. Due to UNIX compatibility and POSIX compliance, migration of applications to and from this operating system (portability) is easier to achieve;
- A higher-level software (TCP/IP Client Application) that runs in a Unix Workstation.

The development of the software for these three platforms was made mainly in C language due to the facility of use, universality and portability of this type of code. In some cases DSP assembler is being used for performance reasons.

For future development and integration in new Unix Workstation, a software library was developed.

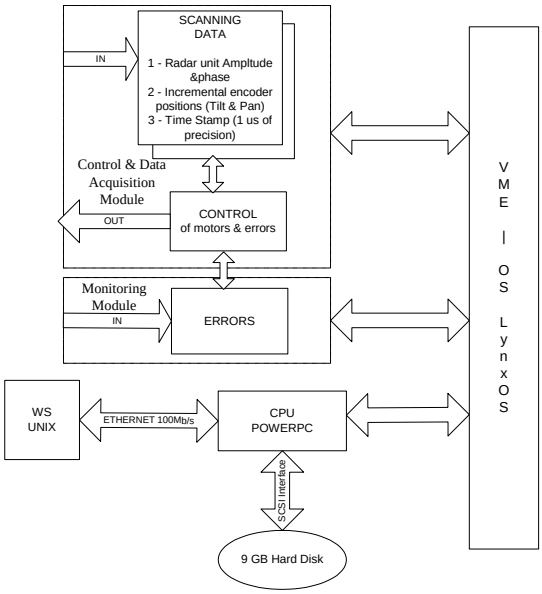

Fig. 9.9 – Block diagram of CADAS